Friction through Dynamical Formation and Rupture of Molecular Bonds

A. E. Filippov,[1] J. Klafter,[2] and M. Urbakh[2]

[1]*Donetsk Institute for Physics and Engineering of NASU, 83144, Donetsk, Ukraine*
[2]*School of Chemistry, Tel Aviv University, 69978 Tel Aviv, Israel*

We introduce a model for friction in a system of two rigid plates connected by bonds (springs) and experiencing an external drive. The macroscopic frictional properties of the system are shown to be directly related to the rupture and formation dynamics of the microscopic bonds. Different regimes of motion are characterized by different rates of rupture and formation relative to the driving velocity. In particular, the stick-slip regime is shown to correspond to a cooperative rupture of the bonds. Moreover, the notion of static friction is shown to be dependent on the experimental conditions and time scales. The overall behavior can be described in terms of two Deborah numbers.

There has been a growing number of attempts to understand the microscopic origin of frictional forces between surfaces in relative motion [1–4]. One of the important areas of investigations that has been somewhat overlooked is that of strongly irreversible tribological processes, which include cold welding, material mixing, and tribochemical and triboelectrical effects. So far only a few experimental investigations [5–7] and molecular dynamics simulations [8–11] have been performed to study these strongly irreversible phenomena at a microscopic scale.

Recent experimental studies of dynamics of cold welds [5] and adhesive boundary lubrication [6] have suggested that macroscopic friction might originate from the formation and rupture of microscopic bonds (junctions) that form between surfaces in close vicinity. Furthermore, these findings indicate that stick-slip motion is connected to a *collective* behavior of the bonds [5]. However, the mechanism underlying this collective behavior is an open issue. In this Letter we propose a microscopic model that establishes a relationship between the dynamics of formation and rupture of individual bonds and macroscopic frictional phenomena. We suggest mechanisms of sliding and stick-slip motions that have been observed in tribological experiments with adhesive boundary lubricated surfaces [6] and cold welding [5]. Here we go beyond the elastic response of the embedded system to include strongly nonlinear rupture effects that contribute essentially to energy dissipation. Closely related models have been proposed earlier [12,13], but the detailed microscopy, its relationship to the macroscopic plate motion, and, in particular, the conclusions are all different.

Figure 1 presents the model investigated in the Letter. The model includes two rigid plates connected by bonds (junctions) that spontaneously break and then reform upon a contact. We model the bonds (N of them) by elastic springs each with a force constant κ and a rest length $l^{(0)}$. The top plate with mass M and center-of-mass coordinate X is pulled with a linear spring of spring constant K. The spring is connected to a stage that moves with a constant velocity V. The motion of the driven plate can be described by the following equation:

$$M\ddot{X} + \eta\dot{X} + F_b + K(X - Vt) = 0, \qquad (1)$$

where

$$F_b = \sum_{i=1}^{N} q_i f_i^{(x)} \qquad (2)$$

is the force due to the interaction between the bonds and the driven plate, and η is a damping coefficient. The parameter q_i characterizes the state of the individual bonds: $q_i = 1$ corresponds to the state of an intact bond that connects the two plates, and $q_i = 0$ corresponds to a ruptured bond that is attached to only one of the plates. The interaction between the plate and the intact bond i is given by the elastic force $f_i = \kappa[l_i - l^{(0)}]$ whose projection in the direction of motion equals $f_i^{(x)} = f_i x_i / l_i$. Here l_i and x_i are the length of the bond and its extension in the X direction correspondingly, $l_i = (x_i^2 + h^2)^{1/2}$, and h is the distance between plates.

The frictional dynamics in the model is governed by two competing processes: (i) bond formation—creation of an interplate junction that tends to inhibit sliding, and (ii) bond rupture—detachment of a spring from one of the plates, a process that helps sliding. As long as a bond is
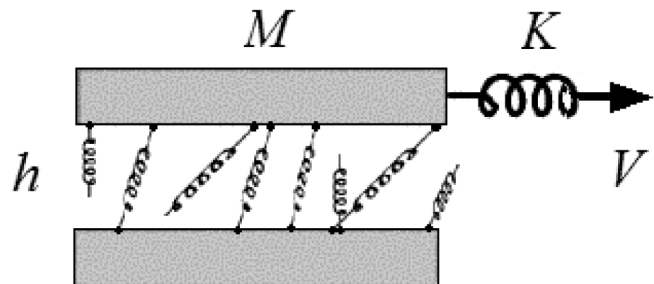
FIG. 1.   Schematic sketch of a model setup.

intact, it is stretched in the lateral direction with the velocity that is equal to the velocity of the top plate, $\dot{x}_i = \dot{X}$, while a ruptured bond relaxes to its equilibrium state. The dynamics of bond stretching and contraction can be described by the following equation:

$$\dot{x}_i = q_i \dot{X} - \lambda(1 - q_i)x_i, \qquad (3)$$

where λ is a relaxation constant that describes the approach of a spring to its equilibrium length. Notice that bond stretching is renewed every time the contact reforms and, thus, the lengths and elastic forces are different for different bonds.

Equations (1)–(3) should be supplemented by an equation that governs rupture and formation of bonds and defines the time dependence of the state parameter, q_i. This equation can be written as

$$q_i(t + \Delta t) = q_i(t) - q_i(t)\theta(\xi_i - \Delta t k_{\text{off}})$$
$$+ [1 - q_i(t)]\theta(\xi_i - \Delta t k_{\text{on}}), \qquad (4)$$

where Δt is a time step in our calculations, ξ_i is a random variable chosen from the interval $(0, 1)$, and $\theta(z)$ is a Heaviside step function that accounts for a stochastic rupture (formation) of a bond that occurs for $\xi_i < \Delta t k_{\text{off(on)}}$. The rates of these processes are given by k_{off} and k_{on} correspondingly.

A bond rupture can be considered as a thermally assisted escape from a bound state over an activation barrier $\Delta E(l_i)$, which is spring-length dependent and diminishes as the applied elastic force, f_i, increases (the bond is stretched) [14–17]. Below we use two approximations for the rupture rate, $k_{\text{off}}(l_i)$, which are appropriate for the cases of weak bonds (the bond energy is only slightly larger than $k_B T$) and of strong bonds (the bond energy $\gg k_B T$) [14–17]. In the first case the time-dependent dissociation rate takes the form [16]

$$k_{\text{off}}(l_i) = k_0 \exp(\beta f_i \Delta x), \qquad (5)$$

while for the strong bonds we use [17]

$$k_{\text{off}}(l_i) = k_0(1 - f_i/f_c)^{1/2} \exp\{-\beta[U_0(1 - f_i/f_c)^{3/2} - U_0]\}. \qquad (6)$$

Here k_0 is the spontaneous rate of bond dissociation in the absence of the external force, and Δx is the distance between the minimum and the maximum of the reaction potential, U_0 is the depth of the potential, f_c is the critical force at which the potential barrier vanishes and unbinding occurs in the absence of thermal fluctuations, and $\beta = 1/k_B T$. Equation (5) assumes that the steady increase in the pulling force produces a small constant bias that reduces the height of the potential barrier. Equation (6) takes into account that for a high barrier a bond rupture occurs preferentially when the bond is close to its slippage condition.

The formation, or rebinding, process is characterized by the rate k_{on}. We assume for simplicity that this rate is not affected by the bond length. However, we assume that the probability of a bond formation depends on the "age" of the contact, τ [1,18]. This age, τ, is defined as the time during which the free end of the bond is exposed to a contact area that moves with respect to the bond. To include the effect of the contact age we introduce a characteristic time scale of the contact time, τ_0, needed for a bond formation and assume that the rate of bond formation depends continuously on the time difference $\tau - \tau_0$,

$$k_{\text{on}} = k_{\text{on}}^0 g[(\tau - \tau_0)/\Delta\tau]. \qquad (7)$$

Here k_{on}^0 is the rate of bond formation for an immobile contact, g is a "smeared" stepwise function ($g = 0$ for $\tau \ll \tau_0$ and $g = 1$ for $\tau > \tau_0$), and σ is a width of the function g. The contact time, τ, is inversely proportional to the velocity of the driven plate, $\tau = a/\dot{X}$, where a is a typical length scale of the contact. The time scale τ_0 defines a critical velocity, $V_0 = a/\tau_0$, above which the bond formation becomes improbable. We find that taking into account the contact time in the process of bond formation is a *necessary* condition to obtain stick-slip motion within our model.

We now discuss results obtained for a large number of bonds, $N > 300$, where the measurable frictional forces are proportional to N. In all figures the distances, time, velocities, and forces are presented in units of h, M/η, $h\eta/M$, and $k_B T/h$, respectively.

Our simulations demonstrate that the model exhibits three different regimes of motion: two sliding regimes and a stick-slip motion between them (see Figs. 2 and 3). These regimes can be easily distinguished in Fig. 3(a), which shows the time-averaged maximal and minimal values of the spring forces, $F = K(X - Vt)$, as a function of the driving velocity. These values coincide in the sliding regimes (Sl), but differ in the velocity interval corresponding to the stick-slip regime (SS). The dynamical behavior depicted in Fig. 3(a) has been recently observed in surface forces apparatus experiments with adhesive surfactant surfaces [6].

Low-velocity sliding regime.—Figure 2(a) shows a time series of the spring force and the corresponding fraction of intact bonds, ν_{int}, in the very low-velocity sliding state. This state corresponds to a close-to-equilibrium situation where the rupture of bonds is determined by a spontaneous (thermal) bond dissociation rather than by the effect of shear induced stress that leads to a reduction of the activation barrier ΔE. This regime is limited to velocities for which the spontaneous rate of bond dissociation, k_0, is higher than the velocity dependent rate of decrease of the activation barrier, $k_{\text{bar}} = \kappa V \Delta x \beta$, which yields the condition $V < V_c = k_0/(\kappa\Delta x\beta)$. The very low-velocity sliding demonstrates that observation of static
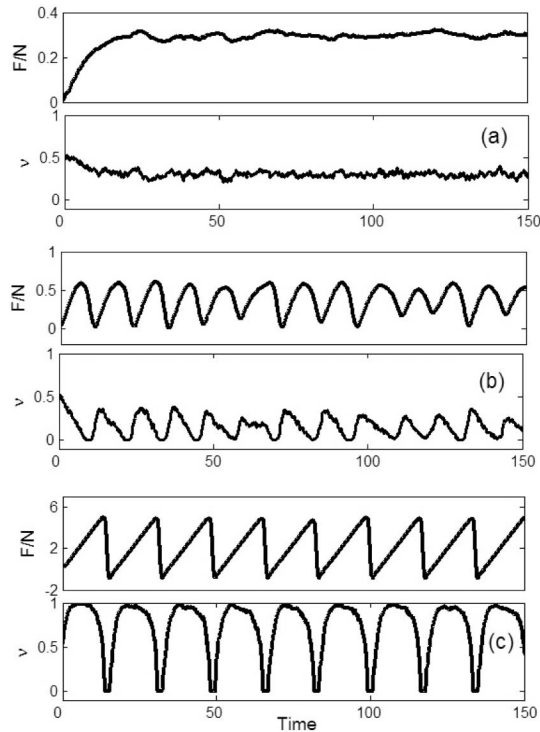
FIG. 2. Time series of the spring force (top panels in each figure) and the fraction of intact bonds (bottom panels) calculated for the model of weak (a),(b) and strong (c) bonds. (a) $V = 0.5$, (b),(c) $V = 2$. Parameter values: $N = 300$, $M \propto N$, $\kappa = 10$, $K = 10^{-2}\kappa N$, $h = 0.25N$, $\lambda = 0.4\eta/M$, $l^{(0)} = h = \Delta x = 1$, $k_0 = k_{on}^0 = 0.1$, $V_0 = 0.5$, $\Delta\tau = 0.1$; in (c) we used $U_0 = 10$, $f_c = 10$, and $k_0 = 0.1\exp(-U)$.

friction depends on the competing external and internal time scales. The definition of static friction should therefore include the experimental time scales.

Our calculations show that the low-velocity sliding actually corresponds to an atomic-scale stick-slip motion of individual bonds. This behavior is clearly seen in Fig. 4(a), which presents the time dependence of an individual bond length and of the ensemble averaged length of the intact bonds. Another characteristic feature of the sliding regime is the essential absence of correlation between individual rupture events, which is again a manifestation of thermal bond dissociation. Figure 4(a) also demonstrates that in spite of strong fluctuations in individual bond length, the ensemble averaged bond length remains constant as a function of time, and it only slightly exceeds the equilibrium bond length.

The model includes two channels of energy dissipation: the first one is related to the rupture and the consequent relaxation of the bonds, and the second is the viscous dissipation, which is given by the term $\eta\dot{X}$ in Eq. (1). The bold solid line in Fig. 3(b) shows the velocity dependence of the kinetic frictional force, $F_k = \int_0^{\Delta t} K(X - Vt)\,dt/\Delta t$, $\Delta t \to \infty$. This gives the net energy dissipated per a unit length passed by the top plate. The rupture and viscous components of the energy dissipation are shown
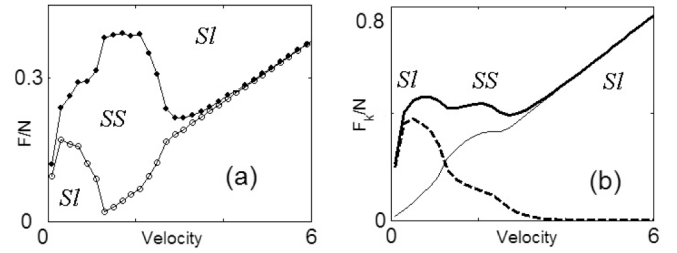
FIG. 3. Velocity dependence of time-averaged frictional forces in the case of weak bonds. (a) Maximal (closed circles) and minimal (open circles) spring forces calculated within the microscopic model for weak bonds. (b) The net kinetic friction (bold line), rupture (dashed line), and viscous (thin line) components of the friction force. Parameter values as in Fig. 2. The symbols Sl and SS indicate sliding and stick-slip regions correspondingly.

by the dashed and thin solid lines, respectively. We see that in the low-velocity sliding regime the energy dissipation is completely dominated by the rupture processes. Then the kinetic frictional force can be estimated taking into account that, being in the intact state, a bond elongates on average by a length $\approx V/k_0$. The latter gives $F_k \approx \kappa VN\langle\nu_{\text{int}}\rangle/k_0$, where $\langle\nu_{\text{int}}\rangle$ is a time-averaged fraction of the intact bonds. In this regime $\langle\nu_{\text{int}}\rangle$ does not depend of the driving velocity and is close to its equilibrium value, $k_{\text{on}}/(k_{\text{on}} + k_{\text{off}})$.

Stick-slip motion.—In the interval of driving velocities $V_0 \gtrsim V \gtrsim V_c$ the model exhibits stick-slip behavior as is seen in Figs. 2(b), 2(c), and 3(a). For the velocities $V \approx V_c$ where processes of spontaneous and shear induced bond dissociation compete, $k_{\text{bar}} \approx k_0$, we observe an erratic stick-slip motion. The stick-slip motion becomes regular under the condition $V_0 > V \gg V_c$, where the rupture is completely determined by the effect of shear stress on the height of the activation barrier [see Fig. 2(c)]. A transition from a sliding to a stick-slip motion is
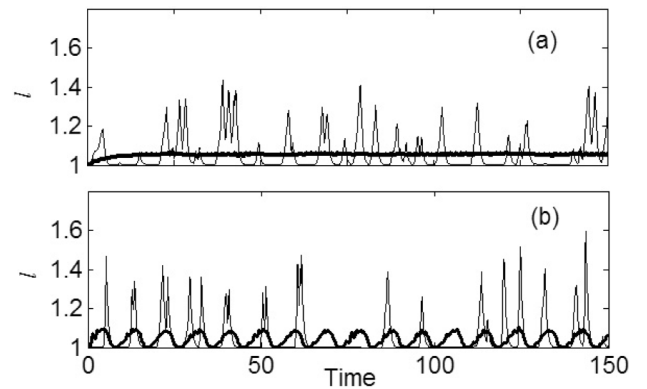
FIG. 4. Time series of an individual bond elongation (thin line) and of the ensemble-averaged bond elongation (bold). (a) $V = 0.5$ corresponding to uncorrelated rupture and (b) $V = 2$ corresponding to collective rupture. Parameter values as in Fig. 2.

accompanied by a decrease of the time-averaged fraction of intact bonds that leads to a decrease of the rupture contribution to the energy dissipation. This effect is balanced by a growth of the viscous component of the energy dissipation [see Fig. 3(b)]. As a result, the kinetic friction depends only slightly on the velocity in the stick-slip regime.

In contrast to the low-velocity sliding regime where rupture events are uncorrelated, the stick-slip motion is characterized by a cooperative behavior of bond subsystem that is clearly visible in Figs. 2(b), 2(c), and 4(b). As more and more bonds break, the force on the remaining ones increases and the bond rupture becomes synchronized. The cooperative rupture of bonds is followed by a time window of a "slip" motion where rebinding is suppressed because of the rather high velocity of the sliding top plate, $\dot{X} \gtrsim V_0 = a/\tau_0$. This simple type of cooperativity arises even in the absence of direct interaction between bonds. Recently, a correlation between macroscopic frictional properties and a collective behavior of microscopic bonds has been observed experimentally [5].

The time-averaged maximal spring force, $F_{\max}$, that corresponds to a synchronized bond rupture can be calculated analytically using a dependence of the rate of rupture, k_{off}, on the external force, Eqs. (5) and (6). For the cases of weak and strong bonds, we get the following dependencies of $F_{\max}$ on the driving velocity, $F_{\max} \propto |\ln V|$ and $F_{\max} \propto |\ln V|^{2/3}$, respectively. Similar scaling laws have recently been proposed for interpretation of the results of frictional forces measurements [19–23] and single molecular rupture experiments [16,17]. A possibility of experimental discrimination between the two scaling laws is actively discussed in the literature [21,22].

High-velocity sliding.—For $V \gtrsim V_0$ a transition from stick-slip motion to the high velocity smooth sliding occurs [see Fig. 2(a)]. In this region bond formation becomes impossible due to the short contact time, $\tau < \tau_0$, and friction is completely determined by viscous dissipation so that $F = \eta V$. It should be noted that low and high velocity sliding regimes differ by the rate of energy dissipation ($\kappa N \langle \nu_{\mathrm{int}} \rangle / k_0$ vs η).

To summarize, we have proposed a model that establishes relationships between macroscopic frictional phenomena and the dynamics of formation and rupture of microscopic bonds. The dynamical response of the system can be characterized by two Deborah numbers, $D_e^{(1)} = V/V_c$ and $D_e^{(2)} = V/V_0$, which describe a competition between the rates of bond rupture and formation and the rate of external drive. In the low-velocity sliding regime $D_e^{(1)}, D_e^{(2)} < 1$, in the stick-slip regime $D_e^{(1)} > 1, D_e^{(2)} < 1$, while in the high velocity sliding regime $D_e^{(1)}, D_e^{(2)} > 1$. And now to a point of caution. Other models such as the Tomlinson, single particle, and Frenkel-Kontorova type models [4,24,25], although physically very different, lead to similar dynamical responses of the driven plate. Namely, force measurements alone do not allow one to establish a microscopic mechanism of friction.

[1] B. N. J. Persson, *Sliding Friction, Physical Properties and Applications* (Springer, Berlin, 2000).
[2] M. G. Rozman, M. Urbakh, J. Klafter, and F.-J. Elmer, J. Phys. Chem. B **102**, 7924 (1998).
[3] S. Granick, Phys. Today **52**, No. 7, 26 (1999).
[4] M. H. Muser, M. Urbakh, and M. O. Robbins, Adv. Chem. Phys. **126**, 187 (2003).
[5] R. Budakian and S. J. Putterman, Phys. Rev. Lett. **85**, 1000 (2000); Phys. Rev. B **65**, 235429 (2002).
[6] C. Drummond, J. Israelachvili, and P. Richetti, Phys. Rev. E **67**, 066110 (2003).
[7] E. Gnecco, R. Bennewitz, and E. Meyer, Phys. Rev. Lett. **88**, 215501 (2002).
[8] M. R. Sorensen, K. W. Jacobsen, and P. Stoltze, Phys. Rev. B **53**, 2101 (1996).
[9] J. Belak and I. F. Stowers, in *Fundamentals of Friction: Macroscopic and Microscopic Processes*, edited by I. L. Singer and H. M. Pollock (Kluwer Academic Publisher, Dordrecht, 1992), p. 511.
[10] A. R. C. Baljon and M. O. Robbins, Science **271**, 482 (1996).
[11] O. M. Braun and J. Roder, Phys. Rev. Lett. **88**, 096102 (2002).
[12] Yu. B. Chernyak and A. I. Leonov, Wear **108**, 105 (1986).
[13] B. N. J. Persson, Phys. Rev. B **51**, 13 568 (1995).
[14] A. Schallamach, Wear **6**, 375 (1963); **17**, 301 (1971).
[15] G. I. Bell, Science **200**, 618 (1978).
[16] E. Evans, Annu. Rev. Biophys. Biomol. Struct. **30**, 105 (2001).
[17] O. K. Dudko, A. E. Filippov, J. Klafter, and M. Urbakh, Proc. Natl. Acad. Sci. U.S.A. **100**, 11378 (2003).
[18] F. Heslot *et al.*, Phys. Rev. E **49**, 4973 (1994).
[19] O. K. Dudko, A. E. Filippov, J. Klafter, and M. Urbakh, Chem. Phys. Lett. **352**, 499 (2002).
[20] Y. Sang, M. Dube, and M. Grant, Phys. Rev. Lett. **87**, 174301 (2001).
[21] E. Riedo *et al.*, Phys. Rev. Lett. **91**, 084502 (2003).
[22] S. Sills and R. M. Overney, Phys. Rev. Lett. **91**, 095501 (2003).
[23] M. H. Muser, Phys. Rev. Lett. **89**, 224301 (2002).
[24] G. A. Tomlinson, Philos. Mag. **7**, 905 (1929).
[25] M. G. Rozman, M. Urbakh, and J. Klafter, Phys. Rev. Lett. **77**, 683 (1996); Europhys. Lett. **39**, 183 (1997).